DIRECT NUMERICAL SIMULATIONS OF HIGH SPEED FLOW OVER CAVITY

A. HAMED, D. BASU, A. MOHAMED AND K. DAS
Department of Aerospace Engineering and Engineering Mechanics
University of Cincinnati, Cincinnati, OH

Abstract

Direct numerical simulations are used to investigate the effect of Mach number on the unsteady flow of an open cavity. The implicit solution is obtained for the compressible Navier-Stokes Equations using compact sixth-order spatial differencing coupled with tenth-order implicit filters. Results for transonic and subsonic flow over a two dimensional cavity are presented for the sound pressure level and pressure fluctuation frequencies.

1. Introduction

Future Strike Aircrafts have a requirement for supersonic release of weapons from internal weapons bays. The associated highly unsteady flow features result in the production of noise levels which are unacceptable for operational and safety considerations. Current generation bay spoilers fail to provide adequate acoustic suppression above Mach one. Some degree of acoustic suppression control has been achieved experimentally by stimulating the shear layer spanning the bay with various actuators (Stanek et al. 2000,2001), however optimizing the performance of these devices requires detailed knowledge of the bay flow field.

Grace (2001) conducted a recent review of computational and experimental studies for flow over cavities. Most of the numerical studies were based on the solution of the time dependent Reynolds-Averaged Navier-Stokes equations (RANS). Colonius et al. (1999) used Direct Numerical Simulations (DNS) to study unsteady subsonic flow over two-dimensional cavities, and predicted transition from the shear layer mode to the wake mode as the Mach number and the cavity length to depth ratio increased. Shieh and Morris (2001) used Detached Eddy Simulations (DES) to study subsonic cavity flow. They predicted the wake mode in the two-dimensional but not in the three-dimensional results, and reported better agreement between the predicted pressure fluctuations' frequency and Rossiter's correlation (1964) for the three-dimensional results. Henderson et al. (2000) pointed out that the challenge is to predict the level of oscillation rather than the frequency of the discrete tones, and presented experimental results for Sound Pressure Level (SPL) at the cavity floor.

Direct numerical simulations are used in the current investigation to study transonic flow over two-dimensional cavities. The results obtained using high order compact differencing in conjunction with high order non-dispersive filters, are presented for the pressure fluctuations, and sound pressure level spectra at the cavity opening for three Mach numbers. The computed vorticity and Mach number contours illustrate the roll up vortex structure in the shear layer and the shock waves above the shear layer as the free stream Mach number increases.

2. Methodology

Direct numerical solutions were obtained for the full compressible Navier-Stokes equations using FDL2DI, the solver developed by Gaitonde and Visbal (1998). The spatial derivatives are represented by high order (up to six) compact approximation that is used in conjunction implicit compact high order filter (up to ten). The scheme achieves second order temporal accuracy using a time-implicit approximately-factored scheme, and Newton-like subiterations. The solver was thoroughly validated by Visbal and Gaitonde (1998,1999) for subsonic flows, wall jets, and acoustic fields. Rizzetta and Visbal (2001) used the code with a third order Roe upwind biased evaluation of the fluxes in the regions of strong shock waves, to perform Large-eddy simulations of supersonic compression-ramp flows.

In the present investigation a sixth-order compact formula was used in the interior points with fifth and fourth orders near the boundary (C45654), according to Visbal and Gaitonde (1999). Similarly the implicit filtering scheme denoted $F10^{0.3}$-0.2.4.6.8.10, was tenth order in the interior with a free parameter $\alpha_f = 0.3$. The equations were normalized using the cavity depth, free stream velocity, and free stream density. The unsteady solution was advanced using implicit time marching with a non-dimensional time step of 2.0 x 10^{-3}. The computational domain for the L/D =2 cavity allowed the laminar boundary layer to develop from uniform free stream conditions at the upstream boundary on the flat plate, which extended 4.95D upstream of the cavity's forward bulkhead. At the upper boundary, which was placed 9.35D above the cavity opening, characteristic conditions were applied for subsonic free stream, and first order extrapolation was applied for supersonic free stream. At the downstream boundary, which was placed at 10.41D behind the rear bulkhead, first order extrapolation was applied. The computational grid included 143x129 points inside the cavity, and 330x95 points on and above the plane of cavity opening. The grid was clustered with a minimum spacing of 1.0 x 10^{-4} D in the streamwise and normal directions.

4. Results and Discussions

Results are presented for a Re_L = 3,000 based on the cavity length, and L/θ = 52.8, where θ is the momentum thickness of the incoming laminar boundary

layer. Sample computational results from the direct numerical simulations are presented for free stream Mach numbers of 1.1, 0.9 and 0.6. The vorticity contours of figure 1 show the roll up vortical structures in the shear layer and the counter rotating vorticity (opposing sign to the boundary layer) near the cavity walls and floor. Figure 1 shows that the vortex size increases with the free stream Mach number, but such large scale shedding as reported by Colonius (1999) for subsonic flow in the wake mode was not observed in the present study. Flow separation upstream of the cavity was not observed in Mach 0.6 and 0.9 cases, and was restricted to a very small region in the case of Mach 1.1. The Mach number contours are presented in figure 2 to show the shock wave structure above the shear layer at different times for Mach 1.1.

The pressure fluctuations at the cavity opening, 0.2 L upstream of the rear bulkhead, are presented in figure 3. The free stream Mach number is seen to have a significant effect on the pressure fluctuations amplitude, which at Mach 1.1 is four times that at Mach 0.6. Figure 4 presents the, SPL spectra, calculated from the pressure fluctuations of figure 3 using 65536 sampled points. The variation in computed SPL at the cavity opening with Mach number is presented in Figure 5. Henderson et al. (2000) presented experimental results for SPL at the cavity floor at Mach 0.85, 0.98, and 1.19. Even though the level was higher in the case of L/D=5 cavity, the variation exhibited similar trends with Mach number. The discrete frequencies determined from the spectra are presented in Figure 6, and compared to Rossiter's modified empirical correlation (Hellar et al. 1970). The correlation, which quantifies the coupling of the acoustic and vorticity fields gives the following equation for feedback frequencies:

$$St_m = \frac{f_m L}{U_\infty} = \frac{m - \alpha}{M_\infty \left/ \sqrt{1 + \frac{\gamma - 1}{2} M_\infty^2} + \frac{1}{k} \right.}$$

Where St_m is the Strouhal number, U_∞, and M_∞ are free stream velocity and Mach number, f_m is the resonant frequency corresponding to the m mode. The constants α, and k were determined experimentally to be 0.25, and 0.57 by Heller et al. (1970) for cavities with L/D greater than four. According to Figure 6, the computed frequencies agree within 6% with Rossiter's equation for the first mode, m=1.

5. Conclusions
The presented results for the unsteady two-dimensional flow over a rectangular cavity demonstrated that the direct numerical simulations captured the flow main features including the vortex shedding, shock waves and coupling of the acoustic and vorticity fields. Further investigations are planned for longer cavity at higher Mach numbers with turbulent upstream boundary layer using Large-eddy simulations.

Acknowledgements

References

Colonius, T., Basu, A. J., and Rowley, C. W. (1999) Numerical Investigation of the Flow Past a Cavity. AIAA 99-1912

Gaitonde, D., and Visbal, M. R., (1998) High-Order Schemes for Navier-Stokes Equations: Algorithm and Implementaion into FL3DI, AFRL-VA-TR-1998-3060.

Gaitonde, D., and Visbal, M. R., (1999) Further Development of a Navier-Stokes Solution Procedures Based on High-Order Formulas, AIAA 1999-0557.

Grace, S. (2001) An Overview of Computational Aeroacoustic Techniques Appliedto Cavity Noise Prediction, AIAA 2001-0510.

Heller, H. H., Holmes, G., and Covert, E. (1970). Flow-Induced Pressure Oscillations in Shallow Cavities, AFFDRL-TR-70-104..

Henderson, J., Badcock, K. J., and Richards, B. E. (2000) Understanding Subsonic and Transonic Open Cavity Flows and Suppression of Cavity Tones," AIAA 2000-0658.

Rizzetta, D. P., and Visbal, M. R. (2001) Large Eddy Simulation of Supersonic Compression-Ramp Flows, AIAA-2001-2858.

Rossitter, J.E. (1964). Wind-Tunnel Experiments on the Flow over Rectangular Cavities at Subsonic and Transonic Speeds. Royal Aircraft Establishment Reports and Memoranda No. 3438.

Shieh, C. M., and Morris, Philip, J. (2001) Comparison of two-and three-dimensional turbulent Cavity Flows, AIAA-2001-0511.

Stanek, M. J., Raman, G., Kibens, V., Ross, J. A., Odedra, J., Peto, J.W. (2000) Control of Cavity Resonance Through Very High Frequency Forcing. AIAA 2000-1905.

Stanek, M. J., Raman, G., Kibens, V., Ross, J. A., Odedra, J., Peto, J.W. (2001) Suppression of Cavity Resonance Using High Frequency Forcing – The Characteristic Signature of Effective Devices, AIAA 2001-2128.

Visbal, M. R. and Gaitonde, D. (1998). Direct Numerical Simulation of a Forced Transitional Plane Wall Jet, AIAA 98-2643.

Visbal, M. R., and Gaitonde, D. (1999) Computation of Aeroacoustic Fields on General Geometries Using Compact Differencing and Filtering Schemes, AIAA 99-3707.
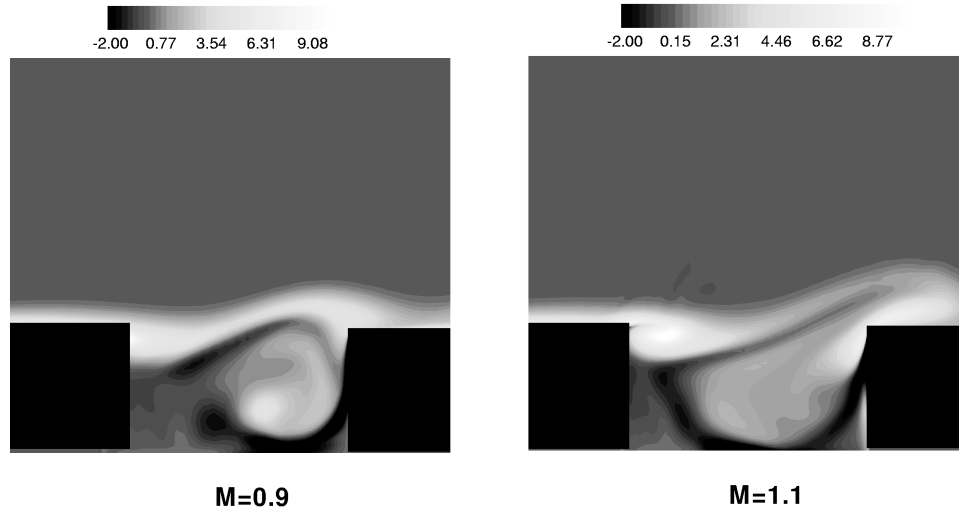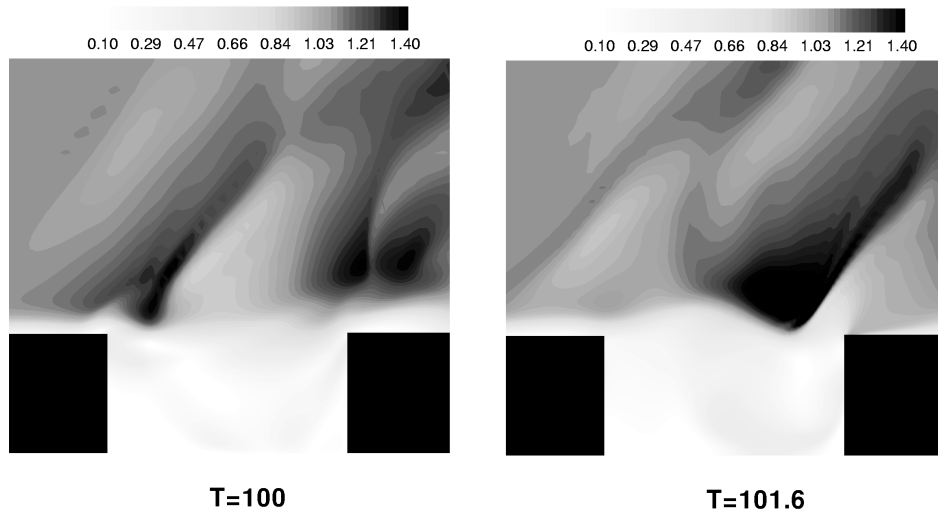
Fig. 1 Vorticity contours

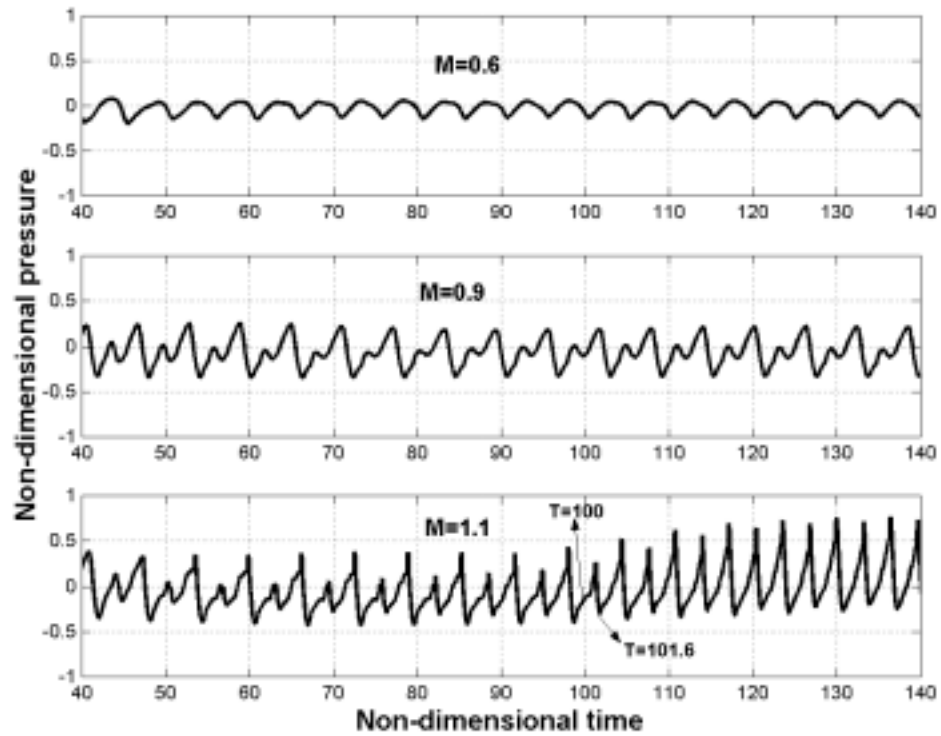Fig. 2 Mach number contours for freestream Mach number 1.1

Fig. 3 Perturbation pressure history at cavity opening for different Mach numbers
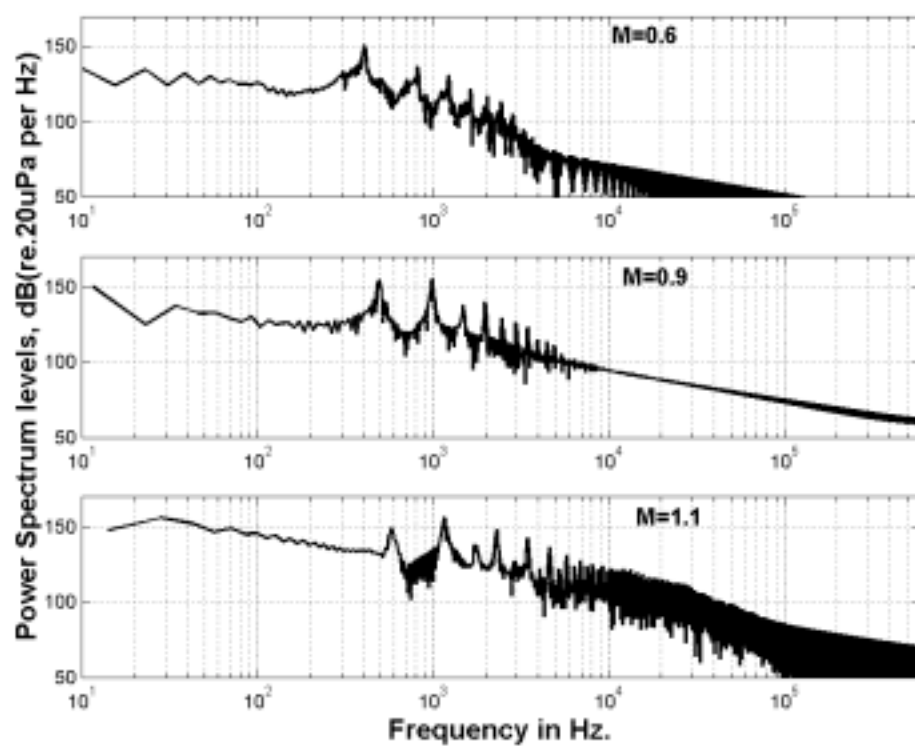
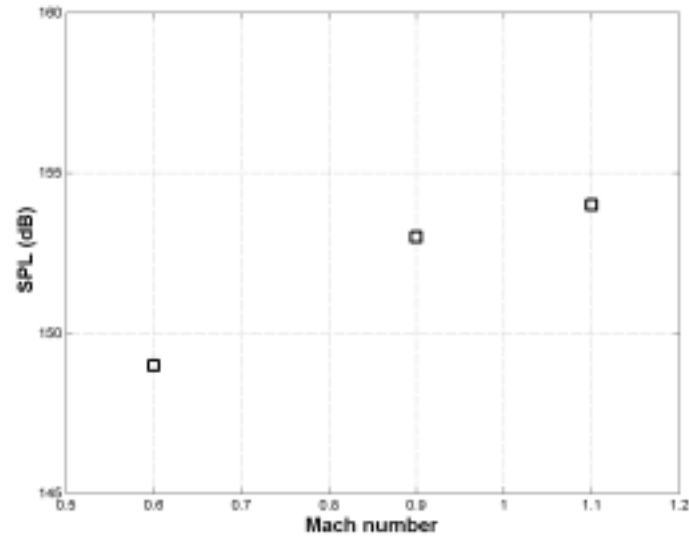Fig. 4 Sound Pressure level (SPL) spectra for different Mach numbers

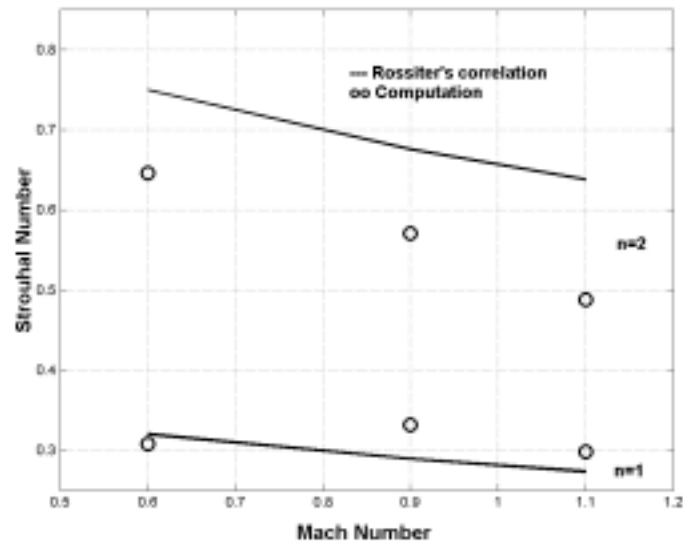Fig. 5 Variation of sound pressure level with Mach number

Fig. 6 Comparison of computed discrete frequencies with Rossiter's correlation